

## Noise and reproducible structure in a GaAs/Al<sub>x</sub>Ga<sub>1-x</sub>As one-dimensional channel

D. H. Cobden, N. K. Patel, M. Pepper, D. A. Ritchie, J. E. F. Frost, and G. A. C. Jones  
*Cavendish Laboratory, University of Cambridge, Madingley Road, Cambridge CB3 0HE, England*  
 (Received 8 March 1991)

We have analyzed the resistance noise, in the time domain, in a GaAs/Al<sub>x</sub>Ga<sub>1-x</sub>As split-gate device showing quantized resistance plateaus. The noise consists mainly of random telegraph signals which can be related to individual slow-electron-trapping defects within the nonconducting regions of the device. These defects are found to influence the conductance mainly by shifting the average electrical potential of the ballistic constriction (channel) relative to the Fermi level. As the gate voltage is varied the defects change their mean occupancy, and this is shown to give rise to some of the reproducible nonquantized structure in the static characteristics of a device. There is clear evidence for interaction between defects.

The quantized plateaus in the resistance of small ballistic constrictions in modulation-doped GaAs/Ga<sub>1-x</sub>Al<sub>x</sub>As systems<sup>1,2</sup> can be flat to within 1% at subkelvin temperatures, but there is often other structure present in the device characteristics.<sup>3</sup> Low-frequency resistance noise is also found in such devices,<sup>4-6</sup> making it difficult to investigate the recently predicted behavior of the shot noise.<sup>7,8</sup> However, the resistance noise itself can yield information about the physics of the system. In this Rapid Communication we discuss measurements in the time domain which help to make clear the nature of this noise and its relationship to the detailed structure in the characteristics.

At the GaAs/Al<sub>x</sub>AsGa<sub>1-x</sub> interface there are spatial potential fluctuations which are due mainly to the random distribution of the remote ionized donors and other defects in the Al<sub>x</sub>Ga<sub>1-x</sub>As and GaAs.<sup>9,10</sup> These fluctuations may cause the transmission coefficients<sup>11</sup>  $T_{ij}$  for the one-dimensional (1D) subbands to differ from those of an ideal smooth, adiabatic system, and possibly to show resonances in transmission or reflection at certain energies, leading to reproducible nonquantized structure in the device characteristics.<sup>12</sup> However, we point out here that such structure also arises as a result of the Fermi-level ( $E_F$ ) dependence of the occupancy of those defects which are able to exchange carriers with the electron gas, and which thereby give rise to resistance noise. As the gate voltage is varied in a split-gate device, the single-electron energy levels of these defects are shifted electrostatically; and as each level passes through  $E_F$  its charge state changes, affecting, in turn, the  $T_{ij}$  and the resistance. Each defect state therefore tends to produce a "bump" in the static characteristics, as we show below, and this mechanism must be allowed for before an attempt is made to relate the structure to resonant behavior of the  $T_{ij}$ .

At a given gate voltage all of the defects having energy levels within a few kT of  $E_F$  are liable to change their charge states randomly in time, resulting in noise in the  $T_{ij}$  and therefore in the resistance. Those that are sufficiently far from the electron gas for their mean electron-capture times to be within the experimental bandwidth may cause random telegraph signals<sup>13,14</sup> (RTSs) in the resistance. In our devices most of the excess noise is clearly due to RTSs. In agreement with Ref.

6 we see no thermal activation of the time constants of the RTSs below 4.2 K, implying that electrons are exchanged by tunneling in this regime. Also, no excess noise is found in the middle of flat plateaus.<sup>4-6</sup> This is simply a consequence of the insensitivity of the quantized resistance to the exact microscopic device parameters.

Here we look in more detail at the gate-voltage dependence of the noise, concentrating on one of the split-gate devices used in Ref. 15. The molecular-beam-epitaxy-grown heterostructure consisted of superlattice buffer, 1- $\mu$ m undoped GaAs, 400- $\text{\AA}$  Al<sub>x</sub>Ga<sub>1-x</sub>As undoped spacer ( $x=0.3$ ), 400- $\text{\AA}$  Si-doped Al<sub>x</sub>Ga<sub>1-x</sub>As, and 200- $\text{\AA}$  GaAs cap. After illumination at 1.2 K the carrier density was around  $3 \times 10^{11} \text{ cm}^{-2}$ , the Fermi energy 10 meV, and the momentum relaxation length in the bulk two-dimensional electron gas (2DEG) 10  $\mu$ m. The geometry of the electron-beam-defined gate metallization is indicated in the inset to Fig. 1. The noise measurements were made using a screened cryostat, at a temperature of 1.2 K, using a four-terminal ac technique with a current of 10 nA and signal frequencies up to 10 kHz. Usually the gate voltage was swept while sampling the externally filtered output of the lock-in amplifier at up to 2 kHz, so obtaining a picture, or "fingerprint", of the noise at each gate voltage superimposed upon the curve of static resistance versus gate voltage.

Shown in Fig. 1 are the static device characteristics measured on one experimental run. The quantized levels for an ideal point contact<sup>16</sup> are indicated by the dashed lines at resistance values of  $h/2ne^2$ , where  $n$  is an integer. Other devices showed the same qualitative behavior in terms of both structure and noise. The average,  $V_g$ , of the voltages on the two sides of the gate was swept here for four fixed values of  $\Delta V_g$ , the difference between these two voltages. The effect of varying  $\Delta V_g$  is principally just to shift the conducting channel transversely,<sup>6,12,17,18</sup> as indicated in the inset to Fig. 1, so altering the local potential landscape and defect environment of the effective ballistic constriction. An analytical calculation based on a highly simplified model of a similar structure<sup>17</sup> predicts that a change of 100 mV in  $\Delta V_g$  should move the center of the channel by something like 70  $\text{\AA}$  in this device, which compares with a classical channel width of about 200  $\text{\AA}$  for

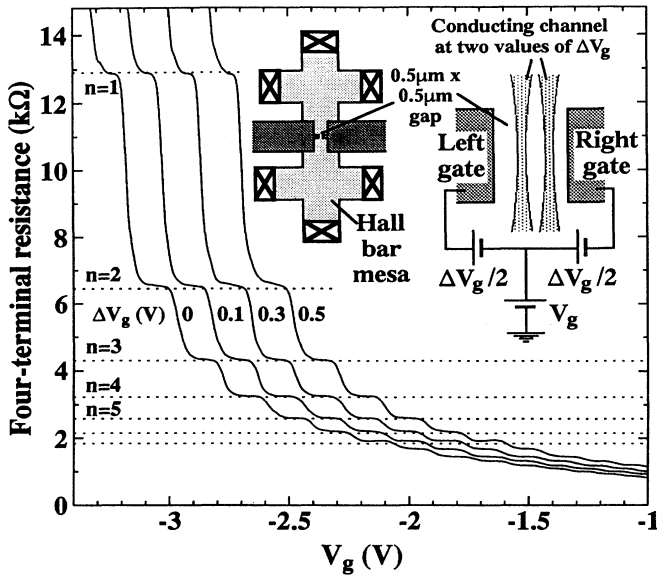


FIG. 1. Static characteristics of a split-gate device at 1.2 K, where  $V_g$  is swept for four fixed values of  $\Delta V_g$ . The curves from left to right are offset in  $V_g$  by 0, 0.15, 0.35, and 0.55 V, respectively. The series resistance of the 2DEG has been subtracted. The schematic inset shows the device geometry and the definitions of  $V_g$  and  $\Delta V_g$ , and indicates the way in which changing  $\Delta V_g$  shifts the conducting channel laterally.

the lowest 1D subband. When  $\Delta V_g$  is changed, or the device is thermally cycled, the characteristics tend to vary in their detailed shape between plateaus and the noise fingerprint may be completely transformed. The noise fingerprint, however, only changes slightly over a few hours at 1.2 K.

For the curves in Fig. 2,  $V_g$  was swept between values corresponding to the  $n=1$  and  $n=2$  resistance plateaus for various values of  $\Delta V_g$ . In each case the noise pattern is different. The clearest feature of the data is probably the way in which the RTSs are seen to switch between members of a set of well defined curves in all cases which we call “quasicharacteristics.” In most cases these are very similar in shape but are displaced from each other along the  $V_g$  axis. If each RTS here is due to a single defect, then the effect of the defect changing its charge state is therefore equivalent purely to that of a change in  $V_g$ . This suggests that the defects are sufficiently far from the constriction that they shift the potential almost uniformly in space relative to  $E_F$ , as assumed in the model of Ref. 6. In this case, in loose analogy with classical discussions of resistance noise,<sup>19</sup> we might say that the defects influence the conducting channel by a “number density” rather than a “mobility” effect, where the latter would here correspond to deviations of the  $T_{ij}$  from their values in a similar but fluctuation-free system. This is supported by the fact that we see no effect of a magnetic field of up to 0.5 T on the amplitude or behavior of the RTSs, implying that the backscattering is not related to a quantum interference process.<sup>20–22</sup>

Concerning the mean time constants of an RTS, denoted by  $t_u$  for the higher-resistance levels and  $t_d$  for the lower-resistance levels, the quantity  $\Sigma = t_u/(t_u + t_d)$  should correspond to the fractional occupancy of the single-electron state involved. If the defect state is in thermal equilibrium with the channel, then  $\Sigma$  should vary from 1 to 0 as  $V_g$  is made more negative and the energy of the state is lifted electrostatically past  $E_F$ . This general behavior is seen for all distinguishable RTSs, but the range of  $V_g$  over which  $\Sigma$  changes can vary greatly. For instance, in the curve at  $\Delta V = -0.2$  V in Fig. 2 the  $V_g$  range

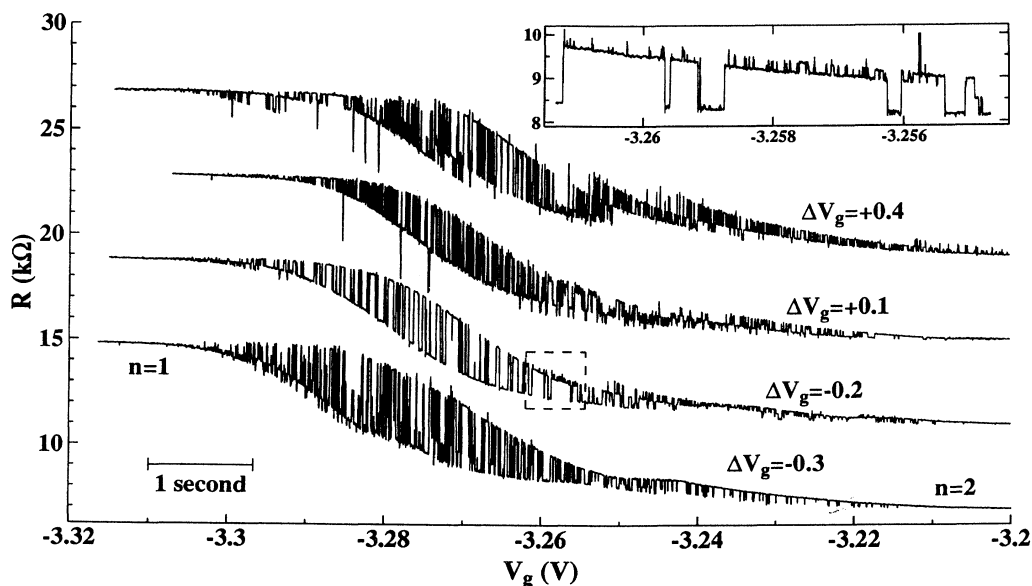


FIG. 2. Portions of the characteristics of the device between the  $n=1$  and  $n=2$  plateaus, measured with a 2-kHz bandwidth at the gate-voltage sweep rate indicated, for four fixed values of  $\Delta V_g$ . The curves are offset by 0, 4, 8, and 12 kΩ from bottom to top, respectively. The inset is an expansion of the dashed box on the sweep at  $\Delta V_g = -0.2$  V.

for the large RTS, which we call RTS1, is comparable with the width of the step, i.e., 60 mV, while for the superimposed small one, RTS2, which is magnified in the inset, the  $V_g$  range is only of order 4 mV. This is consistent with RTS2 being due to a defect that is further from the channel than RTS1, so that it has a smaller influence on the potential at the constriction while its energy level changes more rapidly with  $V_g$  so that it moves more quickly past  $E_F$ .

Note that the way in which the amplitude of RTS2 depends on the state of RTS1 is simply explained as a result of the two defects being noninteracting and characterized by well defined shifts in  $V_g$  of about 11 mV for RTS1 and 2 mV for RTS2. From dc bias measurements on these devices we deduced that the separation of the  $n=1$  and  $n=2$  subbands is around 3 meV,<sup>15</sup> and from this we obtain an estimate of 15 meV/V for the rate of change of the mean potential of the constriction with  $V_g$  in the region of the first two plateaus. Thus the energy shifts of the constriction are about 160  $\mu\text{eV}$  for RTS1 and 30  $\mu\text{eV}$  for RTS2, corresponding to the potentials of point charges in GaAs at distances of 0.7 and 4  $\mu\text{m}$ , respectively. These are, however, likely to be overestimates of the distances to the defects because of screening by the 2DEG and the gate.

The tunneling capture cross section of a defect should decrease as its distance from the electron gas increases. Thus RTSs with narrower  $V_g$  ranges (due to defects that are closer to the gate) might be expected to have longer time constants. In our data, however, we find that  $\tau_u$  and  $\tau_d$  are distributed throughout the experimental bandwidth and have no significant correlation with  $V_g$  range. This is

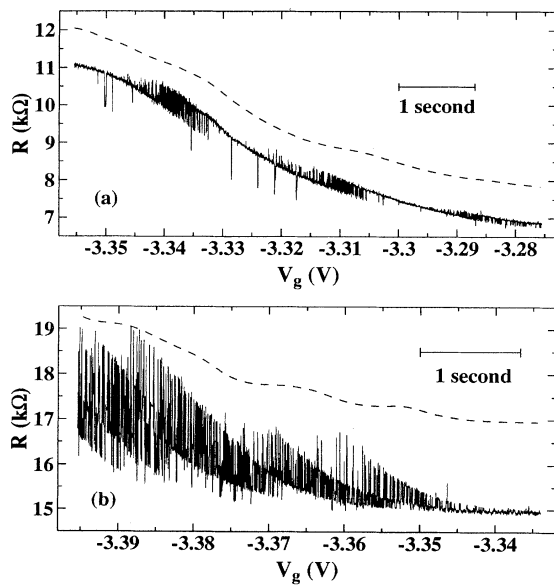


FIG. 3. (a) The solid line is from a sweep of  $V_g$ , for  $\Delta V=0$ , between the  $n=1$  and  $n=2$  plateaus, with a 2-kHz bandwidth and at the indicated speed. The dashed curve is the result of smoothing the same data over 0.2 s, and is vertically offset by 1 k $\Omega$ . A magnetic field of 0.75 T was present. (b) As in (a), but beyond the  $n=1$  plateau and at zero magnetic field, and the dashed curve is offset by 2 k $\Omega$ .

probably due to the distribution of cross sections being influenced by other factors; for instance, there may be several types of defect involved, or the cross section may be highly sensitive to the exact location and atomic environment of a defect.

We now turn to the relationship between RTSs and the structure in the static characteristics. In the full curve of Fig. 3(a), again taken between the  $n=1$  and  $n=2$  plateaus but on another experimental run, the resistance goes through a sequence of RTSs of similar amplitude which change their occupancies over narrow  $V_g$  ranges that do not overlap. In Fig. 3(b), beyond the  $n=1$  plateau, the  $V_g$  ranges of many RTSs overlap and the resistance switches between a set of quasicharacteristics, each presumably corresponding to a different charge configuration of all the defect levels close to  $E_F$ . The smooth dashed curves in the figures are plots of the same data but digitally filtered with Gaussian smoothing widths of 0.2 s, demonstrating how structure can be related to defects with characteristic times that are out of the experimental bandwidth. An isolated bump in the static characteristics may therefore at

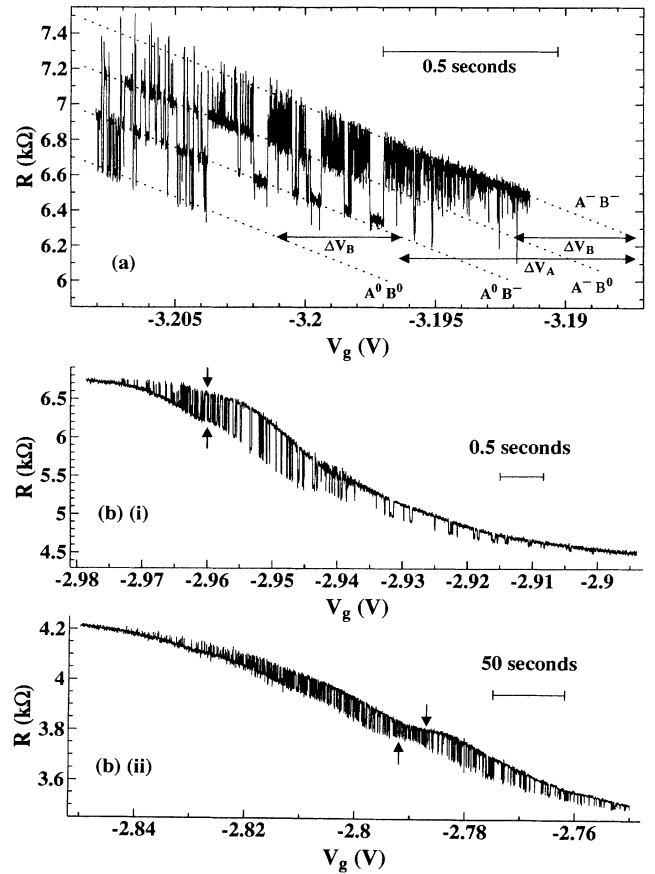


FIG. 4. (a) A portion of a sweep, with a 2-kHz bandwidth, between the  $n=1$  and  $n=2$  plateaus of the device, showing the result of defect interaction (see text). A magnetic field of 0.1 T was present, but the behavior of the RTSs was the same as that at zero magnetic field. (b) The sweep in curve *i* was taken between the  $n=1$  and  $n=2$  plateaus at  $\Delta V_g = +0.2$  V ( $B=0$ ), and that in curve *ii* between  $n=3$  and  $n=4$  at  $\Delta V_g = 0$ .

least sometimes be attributed to a single defect changing its state, while more complex structure may result from the simultaneous activity of many defects. Structure can be seen clearly in the quasicharacteristics of the lower curves in Figs. 2 and 4(b). Note that the rapid evolution of the noise pattern as  $\Delta V_g$  is varied leads to a corresponding evolution of the structure in the static characteristics.

Finally, we discuss defect interactions. Many of the RTSs seen in these devices exhibit complex behavioral patterns that can be explained in terms of electrostatic interactions between defects. The trace in Fig. 4(a) serves as an example. Here we presume that there are two active defects, labeled  $A$  and  $B$ , having charge states  $A^-$ ,  $A^0$ ,  $B^-$ , and  $B^0$ , where  $A^-$  contains one electron more than  $A^0$ , and similarly for  $B^-$  and  $B^0$ . The parallel straight dashed lines were fitted by eye to the quasicharacteristics, which are allocated defect states so that the highest resistance corresponds to  $A^-B^-$  and so on, as indicated. The amplitude of  $B$ 's transition, represented by a shift of  $\Delta V_B$  in  $V_g$ , is independent of the state of  $A$ , whose amplitude is represented by  $\Delta V_A$ . However, the occupancy  $\Sigma_B$  of defect  $B$  is clearly influenced by the state of  $A$ . When  $A$  is in state  $A^0$ ,  $\Sigma_B = 0.5$  at  $V_g \approx 3.208$  V, while when it is in state  $A^-$ ,  $\Sigma_B = 0.5$  at  $V_g \approx 3.198$  V. It therefore appears that the energy level  $E_B$  of defect  $B$  is modified by the trapping of an electron on defect  $A$ , by an amount  $\Delta E_{AB}$  equal to the effect on defect  $B$  of making  $V_g$  about 10 mV more positive. As  $V_g$  is varied,  $\Sigma_B$  should change from 0.1 to 0.9 as  $E_B$  moves through a range of about 4 kT about  $E_F$ , and from the pattern of the transitions between the  $A^-B^-$  and  $A^-B^0$  quasicharacteristics we can relate this

to a range of roughly 20 mV in  $V_g$ . Thus we estimate  $\Delta E_{AB} \approx (10 \text{ mV}/20 \text{ mV}) \times 4 \text{ kT} \approx 0.2 \text{ meV}$ , corresponding to the Coulomb energy of unscreened point charges in GaAs separated by  $0.5 \mu\text{m}$ .

Curves  $i$  and  $ii$  in Fig. 4(b) are examples of situations where an RTS is active over a bump between plateaus. If the bump is due to a faster defect changing state, like defect  $B$  above, and if the charge state of the slower defect influences the energy of the faster one, the position of the bump should be shifted in gate voltage between the two quasicharacteristics of the RTS. In curve  $i$  the bump marked by arrows is at the same value of  $V_g$  in the two quasicharacteristics, implying no significant interaction, while in curve  $ii$  the marked bump is shifted, indicating some interaction. Structure arising from resonances in the  $T_{ij}$  would be expected to shift along with the plateaus between the quasicharacteristics, and possibly to change its shape if the potential landscape is significantly distorted by the slow defect. Thus the bump in curve  $ii$  could have this alternative origin, whereas that in curve  $i$  is very likely to result from a defect changing its state.

We would like to thank Dr. M. J. Uren, Dr. M. J. Kirton, Dr. L. Martin-Moreno, and Dr. D. E. Khmel'nitskii for helpful discussions. This work was supported by the Science and Engineering Research Council and the European Community (EC) under the auspices of EC European Strategic Programme of Research and Development in Information Technology (ESPRIT) basic research action, Grant No. 3043.

- <sup>1</sup>D. A. Wharam, T. J. Thornton, R. Newbury, M. Pepper, H. Ahmed, J. E. F. Frost, D. G. Hasko, D. C. Peacock, D. A. Ritchie, and G. A. C. Jones, *J. Phys. C* **21**, L209 (1988).
- <sup>2</sup>B. J. Van Wees, H. van Houten, C. W. J. Beenakker, J. G. Williamson, L. P. Kouwenhoven, D. van der Marel, and C. T. Foxton, *Phys. Rev. Lett.* **60**, 848 (1988).
- <sup>3</sup>G. Timp, R. Behringer, S. Samperi, J. E. Cunningham, and R. E. Howard, in *Proceedings of the International Symposium on Nanostructure Physics and Fabrication*, edited by W. P. Kirk and M. Reed (Academic, New York, 1989).
- <sup>4</sup>Y. P. Li, D. C. Tsui, J. J. Heremans, J. A. Simmons, and G. W. Weimann, *Appl. Phys. Lett.* **57**, 774 (1990).
- <sup>5</sup>C. Dekker, A. J. Scholten, F. Liefink, R. Eppenga, H. van Houten, and C. T. Foxon, *Phys. Rev. Lett.* **66**, 2148 (1991).
- <sup>6</sup>G. Timp, R. E. Behringer, and J. E. Cunningham, *Phys. Rev. B* **42**, 9259 (1990).
- <sup>7</sup>G. B. Lesovik, *Pis'ma Zh. Eksp. Teor. Fiz.* **49**, 515 (1989) [*JETP Lett.* **49**, 594 (1989)].
- <sup>8</sup>M. Büttiker, *Phys. Rev. Lett.* **65**, 2901 (1990).
- <sup>9</sup>F. Stern, *Appl. Phys. Lett.* **43**, 974 (1983).
- <sup>10</sup>John Nixon and John Davies, *Phys. Rev. B* **41**, 7929 (1990).
- <sup>11</sup>M. Büttiker, *Phys. Rev. B* **41**, 7906 (1990).
- <sup>12</sup>J. G. Williamson, C. E. Timmering, C. J. P. M. Harmans, J. J. Harris, and C. T. Foxon, *Phys. Rev. B* **42**, 7675 (1990).
- <sup>13</sup>K. S. Ralls, W. J. Skocpol, L. D. Jackel, R. E. Howard, L. A. Fetter, R. W. Epworth, and D. M. Tennant, *Phys. Rev. Lett.* **52**, 228 (1984).
- <sup>14</sup>M. J. Kirton and M. J. Uren, *Adv. Phys.* **38**, 367 (1989).
- <sup>15</sup>N. K. Patel, L. Martin-Moreno, M. Pepper, R. Newbury, J. E. F. Frost, D. A. Ritchie, G. A. C. Jones, J. T. M. B. Janssen, J. Singleton, and J. A. A. J. Perenboom, *J. Phys. Condens. Matter* **2**, 7247 (1990).
- <sup>16</sup>R. Landauer, *Z. Phys. B* **68**, 217 (1987).
- <sup>17</sup>L. I. Glazman and I. A. Larkin, *Semicond. Sci. Technol.* **6**, 32 (1991).
- <sup>18</sup>R. J. Stroh and M. Pepper, *J. Phys. Condens. Matter* **1**, 8481 (1989).
- <sup>19</sup>See, for example, B. Pellegrini, *Solid-State Electron.* **29**, 1279 (1986).
- <sup>20</sup>P. A. Lee and D. A. Stone, *Phys. Rev. Lett.* **55**, 1622 (1985).
- <sup>21</sup>G. M. Gusev, Z. D. Kvon, E. B. Olshanetsky, V. Sh. Aliev, V. M. Kudriashov, and S. V. Palesky, *J. Phys. Condens. Matter* **1**, 6507 (1989).
- <sup>22</sup>V. I. Fal'ko and D. E. Khmel'nitskii, *Pis'ma Zh. Eksp. Teor. Fiz.* **51**, 166 (1990) [*JETP Lett.* **51**, 190 (1990)].